ORIGINAL ARTICLE

New osteological and morphological data of four species of *Aphaniops* (Teleostei; Aphaniidae)

Eleni A. Charmpila[1] | Azad Teimori[2] | Jörg Freyhof[3] | Anton Weissenbacher[4] | Bettina Reichenbacher[1,5] [ID]

[1]Department of Earth and Environmental Sciences, Palaeontology and Geobiology, Ludwig-Maximilians-Universität München, Munich, Germany

[2]Department of Biology, Faculty of Sciences, Shahid-Bahonar University of Kerman, Kerman, Iran

[3]Museum für Naturkunde, Leibniz Institute for Evolution and Biodiversity Science, Berlin, Germany

[4]Zoo Vienna, Vienna, Austria

[5]GeoBio-Center, Ludwig-Maximilians-Universität München, Munich, Germany

Correspondence
Bettina Reichenbacher, Department of Earth and Environmental Sciences, Palaeontology and Geobiology, Ludwig-Maximilians-Universität München, Munich, Germany.
Email: b.reichenbacher@lrz.uni-muenchen.de

Abstract

Aphaniops dispar, widespread around the Arabian Peninsula, was recently separated in four species (*A. dispar*, *A. hormuzensis*, *A. kruppi*, *A. stoliczkanus*) by molecular results and colour patterns, but the morphological differences are small and call for more studies. Here we report differences in skeleton and median fin osteology of these species. In addition, we introduce the term 'modified caudal vertebra' to describe caudal vertebrae that are not directly associated with caudal ray support but are visibly modified from a 'usual' caudal vertebra. *Aphaniops hormuzensis*, an endemic species to southern Iran, has a significantly higher number of modified caudal vertebrae compared to the more widespread *A. stoliczkanus* and *A. dispar*, and also to *A. kruppi*. This is a surprising result as the caudal skeleton and related structures of the posterior caudal vertebral column have yielded successful results in separating between families or genera, but there are only a few studies that have examined these structures for their role in species diagnosis. Our study also highlights that state-of-the-art methods in X-raying and improved staining procedures assist in the discrimination of superficially similar species.

KEYWORDS
adaptation, *Aphaniops hormuzensis*, osteology, vertebral column

1 | INTRODUCTION

Aphaniidae is a family of killifishes found only in the Old World which displays a high degree of adaptability to diverse habitats as well as high population divergence rates (e.g. Buj et al., 2015; Cavraro et al., 2017; Ferrito, Mannino, Pappalardo, & Tigano, 2007). Until recently all its representatives were assigned to a single genus, *Aphanius* Nardo, 1827. However, Esmaeili, Teimori, Zarei, and Sayyadzadeh (2020) separated *Aphaniops* Hoedeman, 1951 as well as *Paraphanius* Esmaeili et al., 2020 as own genera. *Aphanius* and *Paraphanius* have

a geographic distribution along the coasts of the Mediterranean Sea and also occur in inland habitats of Turkey, Jordan, Iran, and Iraq, while *Aphaniops* lives in coastal and inland habitats in the South-Eastern Mediterranean and the Dead Sea basins, the Persian Gulf, and all around the Arabian Peninsula south to Ethiopia and east to India (Esmaeili et al., 2020; Wildekamp, 1993).

The type species of *Aphaniops* is *A. dispar* (Nardo, 1827). It has long been considered to form a species group rather than a single species due to its high phenotypic variation among geographically distant populations (Wildekamp, 1993), and has also been used as a

popular model for studying population divergence (e.g. Coad, 1980; Hrbek & Meyer, 2003; Krupp, 1983; Krupp & Schneider, 1989; Reichenbacher, Feulner, & Schulz-Mirbach, 2009; Teimori, Jawad, Al-Kharusi, Al-Mamry, & Reichenbacher, 2012; Villwock, Scholl, & Krupp, 1983). However, studies by Freyhof, Weissenbacher, and Geiger (2017), Teimori, Esmaeili, Hamidan, and Reichenbacher (2018) and Esmaeili et al. (2020) indicate that *A. dispar* includes four species (*A. dispar*, *A. hormuzensis* Teimori et al., 2018, *A. kruppi* Freyhof et al., 2017, *A. stoliczkanus* (Day, 1872)), which, together with further five species (*A. furcatus* Teimori, Esmaeili, Erpenbeck, & Reichenbacher, 2014, *A. ginaonis* (Holly, 1929), *A. richardsoni* (Boulenger, 1907), *A. sirhani* Villwock et al., 1983, *A. stiassnyae* (Getahun & Lazara, 2001)) comprise the genus *Aphaniops*.

In this study, we focus on *A. dispar* and three species of the genus *Aphaniops* that have recently been described (*A. hormuzensis*, *A. kruppi*) or re-validated (*A. stoliczkanus*) (Freyhof et al., 2017; Teimori et al., 2018). The three species occur at coastal and inland sites adjacent to the Persian Gulf and the Gulf of Oman (Figure 1). *Aphaniops hormuzensis* is restricted to springs and rivers near the Strait of Hormuz in southern Iran; *A. kruppi* is known from a single drainage in Oman, while *A. stoliczkanus* is widespread in the Persian Gulf basin and occurs also along the Indian Ocean up to India (Freyhof et al., 2017; Teimori et al., 2018). All three species are distinguished by mitochondrial characters, their coloration pattern, otolith morphology (in case of *A. hormuzensis*) and number of scale rows at the base of the caudal fin (in case of *A. kruppi* and *A. stoliczkanus*) (Freyhof et al., 2017; Teimori et al., 2018).

The objective of our study is to explore whether additional morphological characters can be found to distinguish *A. dispar*, *A. hormuzensis*, *A. kruppi*, and *A. stoliczkanus*. Moreover, as none of the previous molecular studies had included both *A. kruppi* and *A. hormuzensis*, we aimed to generate a molecular tree that includes each of the species studied here. For the morphological study, we put a special focus on the osteology of the caudal skeleton, posterior vertebral column, and median fins, which has previously solely been studied in *A. hormuzensis* (see Motamedi, Shamsaldini, Teimori, & Askari Hesni, 2018). Furthermore, we examined whether some of the osteological characters suggested for taxonomic purposes for species of *Pampus* (Stromateidae, Perciformes; see Jawad & Jig, 2017) and for species of the Tripterygiidae (Blenniiformes; see Jawad, Fricke, & Näslund, 2018) could also be suitable for discrimination among the here studied species. In addition, we examined some traditionally used morphometric and meristic characters. For additional comparison, we used *A. furcatus*.

2 | MATERIALS AND METHODS

2.1 | Species studied

Table 1 presents the species and numbers of specimens used in this study and details of the sites where they were collected. *Aphaniops dispar* was available from an aquarium-bred population of which the origin was Jeddah in the Red Sea (F2 generation). Specimens of *A. furcatus* and *A. hormuzensis* were caught at Khurgo in the Hormuzgan Basin (southern Iran, Figure 1). Specimens of *A. kruppi* were available from the type locality Al Mudayrib (aquarium-bred F1 generation) and two further sites in Oman (Table 1, Figure 1). *Aphaniops stoliczkanus* was captured from Mirahmad in the Helleh Basin (southern Iran) and from Al Juwayf in Oman (Figure 1). The sampling complied with protocols approved by the responsible governmental authorities (according to the countries where the sampling was conducted). *Aphaniops dispar*, *A. hormuzensis*, *A. kruppi*, and *A. stoliczkanus* were identified based on their *Cytb* (see below) or CO1 genes (data of J.F.). Individuals of *A. furcatus* were identified by their phenotype (scaleless).

FIGURE 1 Sampling sites (stars) of the studied *Aphaniops* species in Southern Iran and Oman. Inset indicates location of Persian Gulf and Gulf of Oman. Map data @2019 Google

TABLE 1 Specimen numbers and standard lengths (SL) of the *Aphaniops* species used in this study and details of sampling sites

Species	N [n/n]	SL (in mm) range (mean)	Habitat, Area, Country	Site and coordinates
A. furcatus	2 [1/1]	21.5–24.0 (22.7)	Hot sulfuric spring, Hormuzgan Basin, Southern Iran	Khurgo, 27°31′34.1″N, 56°28′08.2″E
A. dispar	9 [9/0]	21.0–28.3 (25.0)	Captive-bred, Saudi Arabia, ″middle of the Red Sea″	Al Arbaeen, Jeddah 21°17′26.9″N, 39°06′15.5″E [comment on this site in Freyhof et al., 2017: p. 565]
A. hormuzensis	23 [20/3]	22–36.4 (27.2)	Hot sulfuric spring, Hormuzgan Basin, Southern Iran	Khurgo, 27°31′34.1″N, 56°28′08.2″E
A. kruppi	11 [11/4]	40.6–51.8 (45.3)	Captive-bred (8 specimens)	Al Mudayrib, type locality, 22°36′46″N, 58°40′31″E
		17.1–21.8 (19.3)	Seasonal water pools, Wadi Al Batha, Oman (3 specimens)	
	4 [4/0]	18.3–25.6 (22.7)	Seasonal water pools, Wadi Al Batha, Oman	Wadi Bani Khalid, 22°36′03.3″N, 59°04′55.3″E
	4 [4/0]	23.3–27.6 (25.5)		Falaj, 22°29′08″N, 39°10′43″E
A. stoliczkanus	42 [20/5]	14.4–29.7 (20.9)	Hot sulfuric spring, Helleh Basin, Southern Iran	Mirahmad, 28°46′52.8″N, 51°17′12.77″E
	6 [6/0]	19.5–26.2 (22.6)	Seasonal water pool, Oman	Al Juwayf, 24°54.9′16.7″N, 56°10.5′66.7″E

Note: N, total number of specimens; [n/n], numbers of X-rayed specimens/numbers of cleared and stained specimens; SL is given as range and mean. See Data S1 for details of specimens.

2.2 | Molecular genetic analyses

Three fish individuals of *A. kruppi* were newly prepared for DNA extraction by dissecting approximately 25 mg muscle tissue from their caudal peduncle (captive-bred specimens from the type locality Al Mudayrib, see Table 1). Total DNA was extracted using a commercial DNA extraction kit (DNeasy Tissue Kit, Qiagen) following the manufacturer's protocol. The concentration of isolated DNA was estimated using a Nano Drop spectrophotometer. The DNA was diluted to a final concentration of 100 ng/µl.

The specific primers designed for the amplification of the *cytochrome b* gene were used, i.e., Glu-F (5′AACCACCGTTGTATTCAACTACAA3′) and Thr-R (5′ACCTCCGATCTTCGGATTACAAGACCG3′). The amplification processes were performed as follows: initial denaturation 94°C (2 min), 35 cycles with denaturation at 94°C for 45 s, annealing at 60°C for 1 min, extension at 72°C for 1 min per cycle and a final extension phase at 72°C for 10 min. The polymerase chain reaction (PCR) products were visualized on 1% agarose gel using YTA safe stain. The amplified PCR products were sequenced by Pishgam Biotech Co. Sequences were trimmed and assembled in Geneious R10 (Biomatters) (Geneious, 2018). The new sequences are deposited in NCBI Genbank (www.ncbi.nlm.nih.gov) under accession numbers MT661460– MT661462. Sequences from GenBank were added for *A. dispar*, *A. furcatus*, *A. hormuzensis*, *A. ginaonis*, *A. richardsoni*, and *A. stoliczkanus* to gain a representative data set for the assessment of the phylogenetic position of the studied taxa. Sequences were subsequently aligned using Muscle 3.6 (Edgar, 2004), as incorporated in Seaview, under default settings. After sequence alignment, a 800 bp fragment of the *Cytb* gene was obtained. Maximum-likelihood reconstruction searches of the concatenated dataset were conducted with RAxML v. 7.2.5

(Stamatakis, 2006) using a GTR + G + I model of nucleotide substitution, randomized MP starting trees, the fast hill-climbing algorithm, GTR rates, with CAT approximation of rate heterogeneity and fast bootstrap (2000 bootstrap replicates). Bayesian inference was accomplished by MrBayes v. 3.1.2 program (Ronquist & Huelsenbeck, 2003) using the GTR + G + I model. The resulting tree is shown in Figure 2.

2.3 | Study of the skeleton

With the exception of one specimen of *A. furcatus*, three of *A. hormuzensis*, and 19 juveniles and five adults of *A. stoliczkanus* (Mirahmad), all specimens of each species were X-rayed with a Faxitron Bioptics (LLC-Vision NDT version 2.2.5, 45k.v. and 30 s, housed in the Bavarian State Collection of Zoology). The X-ray images were used to analyse the posterior vertebral column, the caudal skeleton, the median fins, and the meristic characters. In addition, one specimen of *A. furcatus*, three of *A. hormuzensis*, four of *A. kruppi*, and five specimens of *A. stoliczkanus* were cleared and stained for additional visualization of the bone using the protocols of Dingerkus and Uhler (1977) and Taylor and van Dyke (1985), with slight modifications (see Data S1 for specimen details).

The terminology of the caudal skeleton and posterior vertebral column follows Schultze and Arratia (2013). Accordingly, preural vertebrae possess "(…) usually both neural and haemal spines, each of which supports a caudal ray at its distal tip." In Aphaniidae, like

in all Cyprinodontiformes, the penultimate caudal vertebra represents PU2, the preceding caudal vertebra is PU3, then PU4, then (if developed) PU5 (Altner & Reichenbacher, 2015; Costa, 2012a; Parenti, 1981). In addition, the new term 'modified caudal vertebra' (MC) is used for the purpose of this study. It describes a vertebra that has, like a preural vertebra, a visible modification of its neural and/or haemal spine in comparison to a 'usual' (= unmodified) caudal vertebra, but differs from a preural vertebra as it is not supporting a caudal ray. The same terminology and definition are also used by Ghanbarifardi et al. (2020).

In addition, the interdigitation formulae for dorsal and anal fins according to Jawad et al. (2018) are employed with some modifications, since the osteology of *Aphaniops* is not directly comparable with that of Tripterygiidae. In our study, the formulae express the number of pterygiophores inserting into the interneural (or interhaemal) spaces between two consecutive neural (or haemal) spines. In the case of the anal fin formula, the haemal spine of the first caudal vertebra is noted with "C" and the number preceding it signifies the number of pterygiophores anterior to it.

Meristic counts of dorsal and anal fin rays follow Holčík (1989) and include every detectable ray that is supported by a pterygiophore. Caudal ray counts include principal caudal rays as well as dorsal and ventral procurrent rays, following Schultze and Arratia (2013). Vertebrae counts comprise abdominal and caudal vertebrae; the latter includes the terminal centrum (TC). Additionally, following Birdsong (1988) the numbers of anal fin pterygiophores (AP) anterior to the first haemal spine are counted.

FIGURE 2 Maximum-likelihood tree of the studied *Aphaniops* species. Colors refer to the individual clades of the *A. dispar* species complex, clade names are adapted from Teimori et al. (2018) (except for *A. kruppi*). Numbers at branches are (from left to right): Maximum-likelihood bootstrap support values on 2000 bootstrap replicates/Bayesian posterior probabilities. Terminal nodes are named as follows: Species name, site, access number in GenBank, country
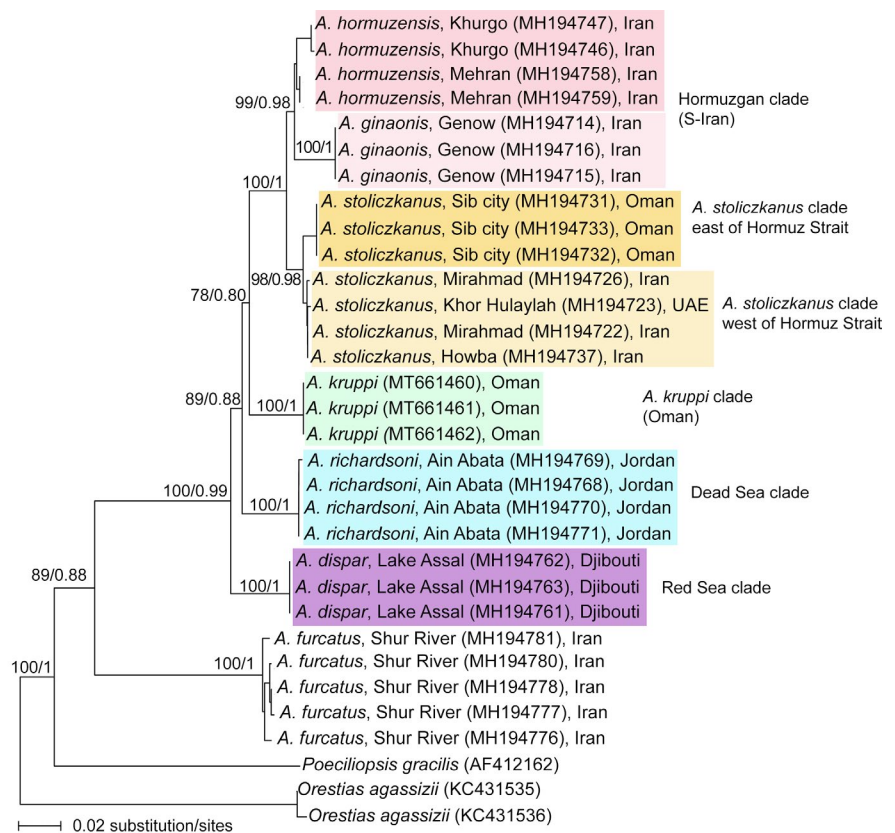
2.4 | Fish morphometry

Six morphometric characters are measured following Holčík (1989). These are standard length (SL), head length (HL), horizontal eye diameter, pre-dorsal length (from the tip of the snout to the dorsal-fin origin), pre-anal length (from the tip of the snout to the anal-fin origin), and length of dorsal fin base. All measurements were taken under a stereomicroscope with a digital caliper with 0.01 mm precision and are expressed as percentage (%) of SL or HL to facilitate species comparisons independent from the size of the specimens.

2.5 | Statistical analyses

Statistical analyses of the morphometric and meristic data were performed with SPSS vers. 26.00 (IBM Corp., 2019). Data from juveniles (SL < 20 mm) were excluded. In addition, _A. furcatus_ and _A. stoliczkanus_ from Al Juwayf were not incorporated in the statistical analyses because their specimen numbers were too low. The specimens of _A. kruppi_ were merged (except for those smaller than 20 mm). For each species, normal distribution of morphometric measurements was tested using Shapiro-Wilk's test ($p < .05$, if non-normal). Morphometric measurements were also tested for covariance with SL (Pearson and Spearman's test, $p > .05$, if no correlation). When covariance was present, morphometric differences between species were explored based on univariate analyses using ANCOVA with Bonferroni correction and SL as covariate (Bonferroni, $p < .05$); otherwise ANOVA with _post-hoc_ tests (Duncan for homogeneous variances and Tamhane's T2 for heterogeneous variances) was used. An exception was HL (%SL) for which we used the Kruskal-Wallis-test because it was not normally distributed in the studied species. Non-normally distributed morphometric measurements and meristic counts (which are per se not normally distributed) were tested for differences among species with non-parametric tests (Kruskal-Wallis test, $p < .05$).

3 | RESULTS

3.1 | Phylogenetic analysis

Phylogenetic analysis was estimated based on the 29 _Cytb_ sequences of the seven _Aphaniops_ species. The three sequences for _A. kruppi_ were newly prepared for this study and 26 sequences were retrieved from GenBank (see Figure 2 for all GenBank accession numbers). Based on the Maximum-likelihood and Bayesian-likelihood analyses, five clades could be recognized, which all were supported by high bootstrap support values (Figure 2). The oldest clade contains _A. furcatus_ from southern Iran and the second clade comprises _A. dispar_ from the Red Sea Basin. The third and fourth clades include _A. richardsoni_ from the Dead sea Basin (Ain Abata, Jordan), and _A. kruppi_ from Oman, respectively. The remaining clade contains three taxa: _Aphaniops stolizckanus_ from southern Iran + Oman is sister to _A. ginaonis_ + _A. hormuzensis_ from the Hormuzgan Basin in southern Iran (Figure 2). It should be noted that the two subclades of _A. stolizckanus_ from Oman (=east of Hormuz Strait) and southern Iran (=west of Hormuz Strait) are well separated with high bootstrap support values.

3.2 | Osteological results

Representative X-ray images of each species, with depictions of their first abdominal vertebra, first and last caudal vertebra, and anal fin pterygiophores are provided in the Appendix 1. Details on counts and measurements of all specimens are presented in the Data S1.

3.3 | Caudal skeleton

The caudal skeleton of all five species displays a single triangular hypural plate, which supports 9–10 continuously arranged principal
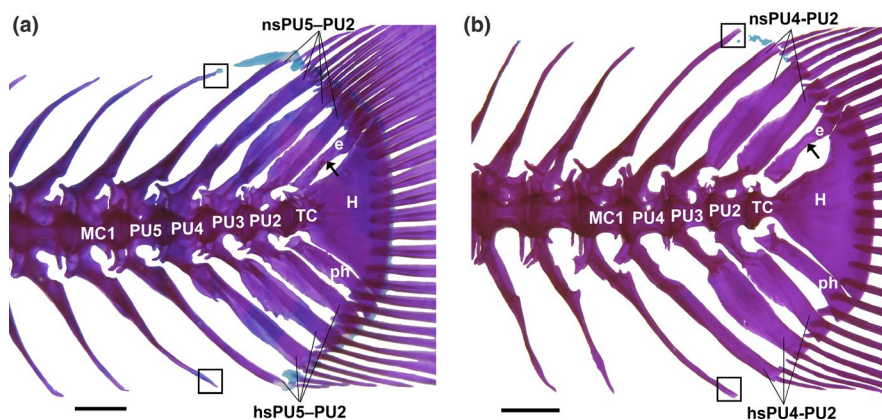

FIGURE 3 Stained caudal skeleton of _A. hormuzensis_ (a, from Khurgo) and _A. stoliczkanus_ (b, from Mirahmad); boxes depict spines of modified caudal vertebra; purple colour depicts bone, light blue indicates cartilage. Abbreviations: e, epural bone, H, hypural plate, hs, haemal spine; MC1, modified caudal vertebra 1; ns, neural spine, ph, parhypural bone; PU, preural vertebra (PU2 is the penultimate vertebra of the vertebral column, the preceding PU is PU3, then PU4, then PU5); TC, terminal centrum. Arrow indicates the constriction in the middle of the epural. Scale bars 0.5 mm

caudal rays. The terminal centrum is fused with the hypural plate (Figures 3, 4). A single epural bone is present in all species; in *A. furcatus* it is thin and straight, whereas in the other four species it is constricted approximately in the middle of its length and slightly widened in its distal part (Figures 3, 4). The parhypural bone is blade-like, straight or slightly bent, with the distal part slightly widened. It is articulated to the terminal centrum in *A. furcatus*, but distant from the terminal centrum in the other four species. The epural and the parhypural bone each supports one to two principal caudal rays.

3.4 | Posterior vertebral column

Three and less frequently two or four preural vertebrae support the caudal rays (Table 2, Figures 3, 4); the neural and haemal spines of the preural vertebra exhibit a constriction and torsion in their proximal part (Figures 3, 4). In *A. furcatus* the spines of the preural vertebrae are thinner and more slender than in the other species; a general reduction in ossification in the skeletal elements occurs in this species.

Anterior to the preural vertebrae, one to three modified caudal vertebrae may be present in all five species. Their neural and/or haemal spines are visibly elongated in comparison to the spine(s) of an unmodified caudal vertebra, but more slender when compared to the spines of the preural vertebrae (Figures 3, 4). We recorded the following configurations of preural and modified caudal vertebrae:

In *A. dispar*, eight (out of nine) specimens display three preural vertebrae (PU2–PU4; Figure 4a), and one specimen has four (PU2–PU5). The specimens with three preural vertebrae present also a single modified caudal vertebra (MC1) (Figure 4a).

In *A. furcatus*, the number of preural vertebrae is two. One or two modified caudal vertebrae are present.

In *A. hormuzensis*, 16 (out of 20) specimens present three preural vertebrae (PU2–PU4), and the remaining specimens have four (PU2–PU5; Figure 3a). The number of modified caudal vertebrae varies from one to three, with two modified caudal vertebrae being the most frequent number (present in 7 out of 20 specimens, Table 2).

In *A. kruppi*, 14 (out of 16) specimens exhibit three preural vertebrae (PU2–PU4), of which 11 also possess a modified caudal vertebra

(Figure 4b). The two remaining specimens display four preural vertebrae (PU2–PU5). The aquarium-bred specimens reveal a more homogeneous caudal skeleton compared to the 'wild' specimens, as both the neural and haemal spine of the modified caudal vertebra are extended, whereas in the 'wild' specimens usually either the neural or the haemal spine of the modified caudal vertebra is visibly longer than the preceding spines of the unmodified caudal vertebrae.

In *A. stoliczkanus* from Mirahmad, all specimens present three preural vertebrae (PU2–PU4) and, except one specimen, one modified caudal vertebra (Figure 3b). In *A. stoliczkanus* from Al Juwayf, all six specimens exhibit three preural vertebrae, but only three of the specimens display also a modified caudal vertebra.

3.5 | Dorsal and anal fin data

The results of the meristic counts are shown in Table 2. The first ray of the dorsal fin is unbranched and supported by two pterygiophores. The first anal fin ray is also unbranched but supported by one pterygiophore. In both fins, the rest of the rays are branched and supported by a single pterygiophore except for the last rays which are not supported by a pterygiophore. The interdigitation formulae of both fins vary to a great degree within and among species. Generalized formulae for each species are shown in Table 3. These formulae present the ranges of pterygiophores in each interneural/interhaemal space from all observed specimens.

3.6 | Morphometric data

The morphometric variables are presented in Table 4 and Figure 5. They were normally distributed with a few exceptions:

- Head length (% SL) for *A. dispar*, *A. kruppi*, *A. stoliczkanus*;
- Standard length for *A. hormuzensis* and *A. kruppi*;
- Pre-dorsal distance (% SL) for *A. stoliczkanus*;
- Pre-anal distance (% SL) for *A. dispar*;
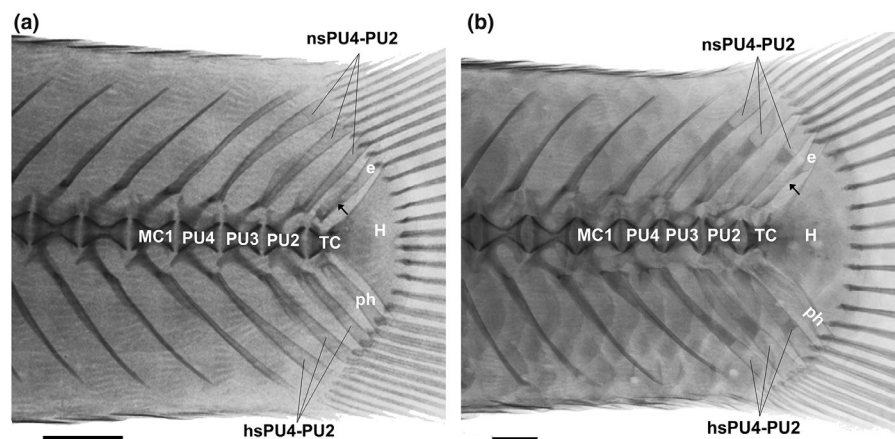- Length of dorsal fin base (% SL) for *A. hormuzensis*

FIGURE 4 X-ray images of the caudal skeleton of *A. dispar* (a) and *A. kruppi* (b). Abbreviations as in Figure 3. Arrow indicates the constriction in the middle of the epural. Scale bars 0.5 mm

TABLE 2 Frequencies of counts of preural vertebrae, modified vertebrae, and meristic characters among the studied species of *Aphaniops*

Counts	Preural vertebrae					Mean ± SD
	3	4				
A. dispar	8	1				3.1 ± 0.3
A. hormuzensis	16	4				3.2 ± 0.4
A. kruppi	14	2				3.1 ± 0.3
A. stoliczkanus	21					3.0 ± 0.0

Counts	Modified caudal vertebrae					Mean ± SD
	1	2	3			
A. dispar	8					1.0 ± 0.0
A. hormuzensis	5	7	6			2.1 ± 0.8
A. kruppi	11					1.0 ± 0.0
A. stoliczkanus	14	1				1.0 ± 0.3

Counts	Principal caudal rays						Mean ± SD
	15	16	17	18	19	20	
A. dispar			2	3	2	2	18.4 ± 1.1
A. hormuzensis	4	8	3	1			16.1 ± 0.9
A. kruppi	4	5	3	3			16.3 ± 1.1
A. stoliczkanus	5	10	1	3			16.2 ± 1.0

Counts	Dorsal procurrent caudal rays					Mean ± SD
	4	5	6	7	8	
A. dispar			3	5	1	6.8 ± 0.7
A. hormuzensis		2	8	6		6.3 ± 0.7
A. kruppi	1	1	8	3	2	6.3 ± 1.0
A. stoliczkanus		1	10	6		6.2 ± 0.6

Counts	Ventral procurrent caudal rays				Mean ± SD
	5	6	7	8	
A. dispar	1		6	2	7.0 ± 0.9
A. hormuzensis	2	9	5		6.2 ± 0.7
A. kruppi	2	8	5		6.2 ± 0.7
A. stoliczkanus	1	11	5	1	6.3 ± 0.7

Counts	Dorsal rays			Mean ± SD
	6	7	8	
A. dispar		5	4	7.4 ± 0.5
A. hormuzensis	5	16	2	6.9 ± 0.5
A. kruppi	9	7		6.4 ± 0.5
A. stoliczkanus	8	14		6.7 ± 0.5

Counts	Anal rays			Mean ± SD
	7	8	9	
A. dispar		4	5	8.6 ± 0.5
A. hormuzensis	2	14	7	8.2 ± 0.6
A. kruppi	1	10	5	8.3 ± 0.6
A. stoliczkanus	3	16	1	7.9 ± 0.5

(Continues)

TABLE 2 (Continued)

Counts	Abdominal vertebrae				
	11	12	13	14	Mean ± SD
A. dispar	1	8			11.9 ± 0.3
A. hormuzensis	2	11	6	1	12.3 ± 0.7
A. kruppi		11	5		12.3 ± 0.5
A. stoliczkanus	2	17	1		12.0 ± 0.4
Counts	Caudal vertebrae				
	13	14	15	16	Mean ± SD
A. dispar			9		15.0 ± 0.0
A. hormuzensis	6	7	11	1	14.6 ± 0.7
A. kruppi		1	14	1	15.0 ± 0.4
A. stoliczkanus		13	10		14.6 ± 0.5
Counts	Anal fin pterygiophores anterior to the first haemal spine					
	1	2	3	4	5	Mean ± SD
A. dispar		7	2			2.2 ± 0.4
A. hormuzensis		10	8		2	2.7 ± 0.9
A. kruppi	1	12	3			2.1 ± 0.5
A. stoliczkanus	5	11	2			1.9 ± 0.6

TABLE 3 Interdigitation formulae for dorsal and anal fins of the studied *Aphaniops* species

Species (n)	Dorsal fin formula	Anal fin formula
A. dispar (9)	1-(0–2)-(1–2)-(1–2)-(1–3)-(1–4)–1*	(2–3)-C-(1–2)-(1–2)-(2–3)-(1–3)
A. hormuzensis (20)	(1–2)-(1–2)-(1–2)-(1–2)-(1–3)-(1–3)*-(1–2)*	(2, 3, 5)-C-(0–2)-(1–2)-(1–3)-(1–3)*
A. kruppi (16)	(1–2)-(1–2)-(1–2)-(1–3)-(1–2)*-(1–2)*	(1–3)-C-(1–2)-(2–3)-(2–3)-(1–3)*
A. stoliczkanus (21)	(1–2)-(1–2)-(1–2)-(1–2)-(1–3)-(1–3)*–1*	(1–3)-C-(0–2)-(1–2)-(1–3)-(1–3)–1*

Note: Data refer to the range of pterygiophores counted within each interneural and interhaemal space from all specimens; *n*, number of examined specimens. The interneural/interhaemal spaces noted with * do not display pterygiophores in all of the studied specimens. In this case, the ranges of the pterygiophores refer only to those specimens that present pterygiophores.

3.7 | Differences between the species

Kruskal-Wallis tests ($p < .05$) indicated different mean values between the species with respect to several characters (Tables 2, 5): The number of modified caudal vertebrae is higher in *A. hormuzensis* (1–3 [2.1 ± 0.8]) versus all other species (1–2 [1.0 ± 0.3]). *Aphaniops dispar* differs significantly from *A. kruppi* and *A. stoliczkanus* in the number of dorsal rays (7–8 [7.4 ± 0.5] in *A. dispar* versus 6–7 [6.4 ± 0.5/6.7 ± 0.5]) and additionally in the number of anal rays from *A. stoliczkanus* (8–9 [8.6 ± 0.5] in *A. dispar* versus 7–9 [7.9 ± 0.5]). Moreover, the number of principal caudal rays is significantly different between *A. dispar* (17–20 [18.4 ± 1.1]) and the rest of the species (15–18 [all approx. 16.2 ± 1.0]). In addition, the number of anal fin pterygiophores anterior to the haemal spine of the first caudal vertebra is significantly different in *A. hormuzensis* (2–5 [2.7 ± 0.9]) versus
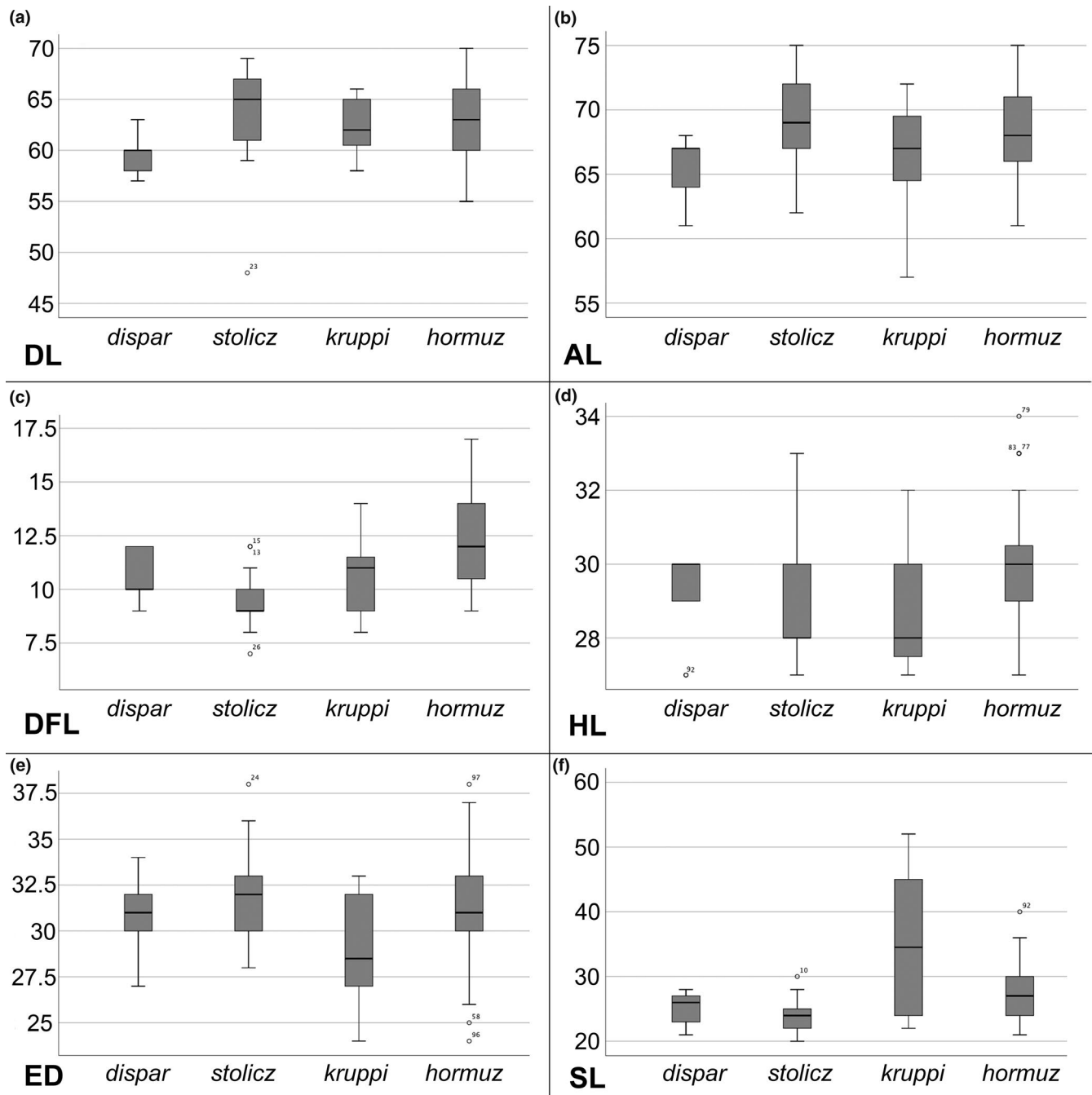
TABLE 4 Morphometric measurements of the studied *Aphaniops* species. Data refer to ranges, mean values, and standard deviation; *n*, number of measured specimens

Species (n)	DL (%SL)	AL (%SL)	DFL (%SL)	HL (%SL)	ED (%HL)
A. dispar (9)	56.9–63.2 (59.8 ± 2.1)	60.9–67.5 (65.6 ± 2.6)	9.1–12.7 (10.6 ± 1.2)	27.2–30.4 (29.1 ± 1.3)	26.8–33.8 (30.9 ± 2.0)
A. hormuzensis (23)	59.0–69.6 (64.0 ± 3.5)	62.5–75.3 (69.09 ± 3.5)	8.7–17.0 (12.4 ± 2.5)	26.6–32.0 (29.7 ± 1.4)	25.3–36.2 (30.6 ± 2.9)
A. kruppi (16)	57.6–65.9 (62.7 ± 3.6*)	57.4–71.8 (68.0 ± 3.7)	8.3–13.6 (11.2 ± 2.3*)	26.7–31.7 (29.4 ± 1.7*)	23.8–33.2 (31.0 ± 3.0*)
A. stoliczkanus (25)	47.7–69.3 (63.5 ± 4.6)	62.3–74.5 (69.5 ± 3.5)	6.8–12.3 (9.4 ± 1.3)	26.7–32.8 (29.1 ± 1.6)	27.5–37.7 (31.9 ± 2.5)

Note: All lengths are expressed in % of standard length (SL), except for eye diameter (ED), which is expressed in % of head length (HL).

Abbreviations: AL, pre-anal length; DFL, length of dorsal fin base; DL, pre-dorsal length.

*Indicates that covariance with SL was detected.

FIGURE 5 Box plots depicting the median (line within box), the 25th and 75th percentiles and the range of the morphometric characters among the studied species of _Aphaniops_. All lengths, except SL and ED, are expressed in % of SL, ED is expressed in % HL. Circles indicate outliers within the 100th percentile. Abbreviations: AL, pre-anal length; DFL, length of dorsal fin base; DL, pre-dorsal length; ED, eye diameter; HL, head length; SL, standard length. Abbreviations for species names: _dispar_, _A. dispar_; _stolicz_, _A. stoliczkanus_; _kruppi_, _A. kruppi_; _hormuz_, _A. hormuzensis_

TABLE 5 Significant differences between species based on pairwise comparisons of meristic and morphometric data (Kruskal-Wallis, $p < .05$, after Bonferroni correction for meristic , ANCOVA, $p < .05$ for morphometric values)

A. dispar vs. A. hormuz.	A. dispar vs. A. kruppi	A. dispar vs. A. stoliczk.	A. hormuz. vs. A. kruppi	A. hormuz. vs. A. stoliczk.	A. kruppi vs. A. stoliczk.
Prirays, MC	Drays, Prirays	Drays, Arays, Prirays	MC, DFL(%SL)	AP, MC, DFL(%SL),	-

Abbreviations: AP, anal fin pterygiophores anterior to first haemal spine; Arays, number of anal rays; DFL, length of dorsal fin base; Drays, number of dorsal rays; MC, number of modified caudal vertebrae; Prirays, number of principal caudal rays (branched + two unbranched); SL, standard length.

A. stoliczkanus (1–3 [1.9 ± 0.6]). Concerning the morphometric data, only the length of the dorsal fin base (% SL) differed significantly between *A. hormuzensis* (8.7–17.0 [12.4 ± 2.5]) versus *A. stoliczkanus* (6.8–12.3 [9.4 ± 1.3]) and *A. kruppi* (8.3–13.6 [11.2 ± 2.3]) (ANCOVA, *p* < .05; Figure 5c). No further significant differences in the morphometric variables could be detected between the species (Figure 5a, b, d–f).

4 | DISCUSSION

One outcome of our study was that the examined specimens of *A. dispar*, *A. hormuzensis*, *A. kruppi*, and *A. stoliczkanus* all exhibited a sinuous and thick epural bone in their caudal skeleton. This characteristic had previously been reported for *A. stoliczkanus* (as *Aphanius dispar* in Costa, 2012a), *A. richardsoni*, *A. ginaonis*, and *A. hormuzensis* (Costa, 2012a; Motamedi et al., 2018; Teimori et al., 2014). Conversely, a sinuous shape of the epural is absent in *A. furcatus* and it is also absent in the related *Paraphanius mento* (this study and Teimori et al., 2014). However, Costa (2012a) reported this character also for *Aphanius isfahanensis*, and two of the Anatolian *Aphanius* species, which are not closely related according to molecular studies (Esmaeili et al., 2020; Hrbek & Meyer, 2003). It could be that this trait has evolved convergently in different clades of the Aphaniidae. Nevertheless, we tentatively propose that a sinuous epural could be the first detected morphological synapomorphy for the 'inner' clade of *Aphaniops*.

Furthermore, we showed that *A. dispar* could be separated from all species based on some meristic counts (Table 5). This confirms its distinctiveness as suggested based on molecular work (Freyhof et al., 2017; Teimori et al., 2018). Concerning the other three species, three of the studied morphological traits were significantly different between *A. hormuzensis* and *A. stoliczkanus*, two characters varied significantly between *A. hormuzensis* and *A. kruppi*, while none of the characters studied here differentiated between *A. kruppi* and *A. stoliczkanus* (Table 5). The interdigitation formulae for the dorsal and anal fins did not reveal a taxonomically useful pattern due to its great variability within each of the studied species (Table 3).

The most conspicuous result was that *A. hormuzensis* revealed an increased number of modified caudal vertebrae (1–3 [2.1 ± 0.8] versus 1–2 [1.0 ± 0.3] in *A. dispar*, *A. furcatus*, *A. kruppi*, and *A. stoliczkanus*). It has previously been reported that the caudal skeleton osteology and the configuration of the posterior caudal vertebral column can facilitate the reconstruction of phylogenetic relations (Arratia & Schultze, 1992; Borden, Grande, & Smith, 2013; Monod, 1968). Furthermore, among killifishes, these structures can play an important role in the discrimination of genera (Altner & Reichenbacher, 2015; Costa, 1998, 2012a, b; Ghedhotti, 2000; Parenti, 1981). However, comparative studies on this structure at the level of species have not been provided in detail for the members of the genus *Aphaniops*. In this study, the newly defined osteological structure of a modified caudal vertebra has proven to be meaningful in species distinctions. In the following, we briefly provide some

hypotheses for the increase of the modified caudal vertebrae number in *A. hormuzensis*, which we think award future consideration.

The caudal skeleton and posterior vertebral columns are functionally associated with the support of the caudal fin, the movement of which can assist the propulsion of a fish in water (Gosline, 1997). Here we hypothesize that the modified caudal vertebrae could have an auxiliary role in reinforcing the support of the caudal fin in *A. hormuzensis*. In addition, we tentatively suggest that the differentiation in the length of the dorsal fin base and the higher number of anal fin pterygiophores anterior to the haemal spine of the first caudal vertebra might enhance the balance of *A. hormuzensis* in the water column, as these two median fins are often linked with such movements that stabilize the fish body in water (see Standen & Lauder, 2005; Tytell, 2006). Whether the observed differences are the result of adaptation, genetic drift - the latter of which has been proposed for *A. hormuzensis* (Teimori et al., 2012) - or an effect of both, is an interesting topic for future research but will require the study of further populations from additional sites.

DATA AVAILABILITY STATEMENT

The new molecular data shown in Figure 2 is available in Genbank (accession numbers MT661460– MT661462). X-ray images of all studied specimens are available upon request to the corresponding author. Collection numbers and details for each specimen are provided in the Data S1.

Data S1: Details of the *Aphaniops* specimens used, their meristic counts from x-rays and the morphometric measurements conducted for this study are available in the Supplementary Dataset that accompanies this paper at https://onlinelibrary.wiley.com/doi/epdf/10.1111/jai.14074.

ORCID

Bettina Reichenbacher https://orcid.org/0000-0001-6678-5080

REFERENCES

Altner, M., & Reichenbacher, B. (2015). †Kenyaichthyidae fam. nov. and †*Kenyaichthys* gen. nov. – First record of a fossil aplocheiloid killifish (Teleostei, Cyprinodontiformes). *PLoS One*, *10*(4), e0123056. https://doi.org/10.1371/journal.pone.0123056

Arratia, G., & Schultze, H.-P. (1992). Reevaluation of the caudal skeleton of certain actinopterygian fishes: III. Salmonidae. Homologization of caudal skeletal structures. *Journal of Morphology*, *214*(2), 187–249. https://doi.org/10.1002/jmor.1052140209

Birdsong, R. S., Murdy, E. O., & Pezold, F. L. (1988). A study of the vertebral column and median fin osteology in gobioid fishes with

comments on gobioid relationships. *Bulletin of Marine Science*, *42*(2), 174–214.

Borden, W. C., Grande, T., & Smith, W. L. (2013). Comparative osteology and myology of the caudal fin in the Paracanthopterygii (Teleostei: Acanthomorpha). In G. Arratia, H.-P. Schultze, & M. V. H. Wilson (Eds.), *Mesozoic Fishes 5 – Global diversity and evolution* (pp. 419–455). München, Germany: Verlag Dr. Friedrich Pfeil.

Buj, I., Miočić-Stošić, J., Marčić, Z., Mustafić, P., Zanella, D., Mrakovčić, M., …Ćaleta, M. (2015). Population genetic structure and demographic history of *Aphanius fasciatus* (Cyprinodontidae: Cyprinodontiformes) from hypersaline habitats in the eastern Adriatic. *Scientia Marina*, *79*(4), 399–408. https://doi.org/10.3989/scimar.04198.06A

Cavraro, F., Malavasi, S., Torricelli, P., Gkenas, C., Liousia, V., Leonardos, I.,…Triantafyllidis, A. (2017). Genetic structure of the South European toothcarp *Aphanius fasciatus* (Actinopterygii: Cyprinodontidae) populations in the Mediterranean basin with a focus on the Venice lagoon. *European Zoological Journal*, *84*(1), 153–166. https://doi.org/10.1080/24750263.2017.1290154

Coad, B. W. (1980). A re-description of *Aphanius ginaonis* (Holly, 1929) from southern Iran (Osteichthyes: Cyprinodontiformes). *Journal of Natural History*, *14*(1), 33–40. https://doi.org/10.1080/00222938000770031

Costa, W. J. E. M. (1998). Phylogeny and classification of the Cyprinodontiformes (Euteleostei: Atherinomorpha): A reappraisal. In L. R. Malabarba, R. E. Reis, R. P. Vari, Z. M. Lucena, & C. A. S. Lucena (Eds.), *Phylogeny and classification of neotropical fishes* (pp. 537–560). Porto Alegre, Brazil: EDIPUCRS.

Costa, W. J. E. M. (2012a). The caudal skeleton of extant and fossil cyprinodontiform fishes (Teleostei: Atherinomorpha): Comparative morphology and delimitation of phylogenetic characters. *Vertebrate Zoology*, *62*(2), 161–180.

Costa, W. J. E. M. (2012b). Oligocene killifishes (Teleostei: Cyprinodontiformes) from southern France: Relationships, taxonomic position, and evidence of internal fertilization. *Vertebrate Zoology*, *62*(3), 371–386.

Dingerkus, G., & Uhler, L. D. (1977). Enzyme clearing of alcian blue stained whole small vertebrates for demonstration of cartilage. *Stain Technology*, *52*(4), 229–232. https://doi.org/10.3109/10520297709116780

Edgar, R. C. (2004). MUSCLE: Multiple sequence alignment with high accuracy and high throughput. *Nucleic Acids Research*, *32*(5), 1792–1797. https://doi.org/10.1093/nar/gkh340

Esmaeili, H. R., Teimori, A., Zarei, F., & Sayyadzadeh, G. (2020). DNA barcoding and species delimitation of the Old World tooth-carps, family Aphaniidae Hoedeman, 1949 (Teleostei: Cyprinodontiformes). *PLoS One*, *15*(4), e0231717. https://doi.org/10.1371/journal.pone.0231717

Ferrito, V., Mannino, M. C., Pappalardo, A. M., & Tigano, C. (2007). Morphological variation among populations of *Aphanius fasciatus* Nardo, 1827 (Teleostei, Cyprinodontidae) from the Mediterranean. *Journal of Fish Biology*, *70*(1), 1–20. https://doi.org/10.1111/j.1095-8649.2006.01192.x

Freyhof, J., Weissenbacher, A., & Geiger, M. (2017). *Aphanius kruppi*, a new killifish from Oman with comments on the *A. dispar* species group (Cyprinodontiformes: Aphaniidae). *Zootaxa*, *4338*(3), 557–573 https://doi.org/10.11646/zootaxa.4338.3.10.

Geneious (2018). *Version R10 created by biomatters*. Retrieved from http://www.geneious.com

Ghanbarifardi, M., Gut, C., Gholami, Z., Esmaeili, H. R., & Gierl, C. & Reichenbacher, B. (2020). Osteology of the posterior vertebral column and caudal skeleton of marine amphibious gobies (mudskippers) (Teleostei: Gobioidei). *Journal of Applied Ichthyology*.1–11. https://doi.org/10.1111/jai.14071.

Ghedotti, M. (2000). Phylogenetic analysis and taxonomy of the poecilioid fishes (Teleostei: Cyprinodontiformes). *Zoological Journal of the Linnean Society*, *130*(1), 1–53. https://doi.org/10.1006/zjls.1999.0213

Gosline, W. A. (1997). Functional morphology of the caudal skeleton in teleostean fishes. *Ichthyological Research*, *44*(2), 137–141. https://doi.org/10.1007/BF02678693

Holčík, J. (1989). *The freshwater fishes of Europe. Vol. 1, Part II. General introduction to fishes Acipenseriformes* (1st ed.). Wiesbaden: AULA-Verlag.

Hrbek, T., & Meyer, A. (2003). Closing of the Tethys Sea and the phylogeny of Eurasian killifishes (Cyprinodontiformes: Cyprinodontidae). *Journal of Evolutionary Biology*, *16*(1), 17–36. https://doi.org/10.1046/j.1420-9101.2003.00475.x

IBM Corp (2019). *IBM SPSS Statistics for Macintosh, Version 26.0*. Armonk, NY: IBM Corp. Retrieved from http://www-01.ibm.com/software/analytics/spss/products/statistics/

Jawad, L. A., Fricke, R., & Näslund, J. (2018). Comparative osteology of the family Tripterygiidae (Teleostei: Blenniiformes). *Journal of the Marine Biological Association of the United Kingdom*, *98*(6), 1487–1511. https://doi.org/10.1017/S002531541700042X

Jawad, L. A., & Jig, L. (2017). Comparative osteology of the axial skeleton of the genus *Pampus* (Family: Stromateidae, Perciformes). *Journal of the Marine Biological Association of the United Kingdom*, *97*(2), 277–287. https://doi.org/10.1017/S0025315416000369

Krupp, F. (1983). Fishes of Saudi Arabia Freshwater Fishes of Saudi Arabia and Adjacent Regions of the Arabian Peninsula. *Fauna of Saudi Arabia*, *5*, 568–636.

Krupp, F., & Schneider, W. (1989). The fishes of the Jordan River Drainage Basin and Azraq Oasis. *Fauna of Saudi Arabia*, *10*, 347–416.

Monod, T. (1968). Le complexe urophore des poisons téléostéens. *Mémoires De L'institut Fondamental D'afrique Noire*, *81*, 1–705.

Motamedi, M., Shamsaldini, F., Teimori, A., & Askari Hesni, M. (2018). Histomicroscopy and normal anatomy of the adult killifish *Aphanius hormuzensis* (Teleostei; Aphaniidae) from the Persian Gulf coastal environment. *Microscopy Research and Technique*, *82*(4), 466–480. https://doi.org/10.1002/jemt.23190

Parenti, L. R. (1981). A phylogenetic and biogeographic analysis of cyprinodontiform fishes (Teleostei, Atherinomorpha). *Bulletin of the American Museum of Natural History*, *168*(4), 335–557.

Reichenbacher, B., Feulner, G. R., & Schulz-Mirbach, T. (2009). Geographic variation in otolith morphology among freshwater populations of *Aphanius dispar* (Teleostei, Cyprinodontiformes) from the southeastern Arabian Peninsula. *Journal of Morphology*, *270*(4), 469–484. https://doi.org/10.1002/jmor.10702

Ronquist, F., & Huelsenbeck, J. P. (2003). MrBayes 3: Bayesian phylogenetic inference under mixed models. *Bioinformatics*, *19*(12), 1572–1574. https://doi.org/10.1093/bioinformatics/btg180

Schultze, H.-P., & Arratia, G. (2013). The caudal skeleton of basal teleosts, its conventions, and some of its major evolutionary novelties in a temporal dimension. In G. Arratia, H.-P. Schultze, & M. V. H. Wilson (Eds.), *Mesozoic fishes 5 – Global Diversity And Evolution*, (pp. 187–246) *5*. München: Verlag Dr. Friedrich Pfeil.

Stamatakis, A. (2006). RAxML-VI-HPC: Maximum likelihood-based phylogenetic analyses with thousands of taxa and mixed models. *Bioinformatics*, *22*(21), 2688–2690. https://doi.org/10.1093/bioinformatics/btl446

Standen, E. M., & Lauder, G. V. (2005). Dorsal and anal fin function in bluegill sunfish *Lepomis macrochirus*: Three-dimensional kinematics during propulsion and maneuvering. *Journal of Experimental Biology*, *208*(14), 2753–2763. https://doi.org/10.1242/jeb.01706

Taylor, W. R., & Van Dyke, G. C. (1985). Revised procedures for staining and clearing small fishes and other vertebrates for bone and cartilage study. [Nouvelle technique de coloration et d'éclaircissement des petits poissons et autres vertébrés pour l'étude de l'os et du cartilage]. *Cybium*, *9*(2), 107–119.

Teimori, A., Esmaeili, H. R., Erpenbeck, D., & Reichenbacher, B. (2014). A new and unique species of the genus *Aphanius* Nardo, 1827 (Teleostei: Cyprinodontidae) from Southern Iran: A case of regressive evolution. *Zoologischer Anzeiger - A Journal of*

Comparative Zoology, *253*(4), 327–337. https://doi.org/10.1016/j.jcz.2013.12.001

Teimori, A., Esmaeili, H. R., Hamidan, N., & Reichenbacher, B. (2018). Systematics and historical biogeography of the *Aphanius dispar* species group (Teleostei: Aphaniidae) and description of a new species from Southern Iran. *Journal of Zoological Systematics and Evolutionary Research*, *56*, 579–598. https://doi.org/10.1111/jzs.12228

Teimori, A., Jawad, L. A. J., Al-Kharusi, L. H., Al-Mamry, J. M., & Reichenbacher, B. (2012). Late Pleistocene to Holocene diversification and historical zoogeography of the Arabian killifish (*Aphanius dispar*) inferred from otolith morphology. *Scientia Marina*, *76*(4), 637–645. https://doi.org/10.3989/scimar.03635.26C

Tytell, E. D. (2006). Median fin function in bluegill sunfish *Lepomis macrochirus*: Streamwise vortex structure during steady swimming. *The Journal of Experimental Biology*, *209*(Pt 8), 1516–1534. https://doi.org/10.1242/jeb.02154

Villwock, W., Scholl, A., & Krupp, F. (1983). Zur Taxonomie, Verbreitung und Speziation des Formenkreises *Aphanius dispar* (Rüppell, 1828) und Beschreibung von *Aphanius sirhani* n. sp. (Pisces, Cyprinodontidae). *Mitteilungen Aus Dem Hamburgischen Zoologischen Museum Und Institut*, *80*, 251–277.

Wildekamp, R. H. (1993). *A world of killies: Atlas of the oviparous cyprinodontiform fishes of the world*, *I*. Mishawaka, Indiana: American Killifish Association.

SUPPORTING INFORMATION

Additional supporting information may be found online in the Supporting Information section.
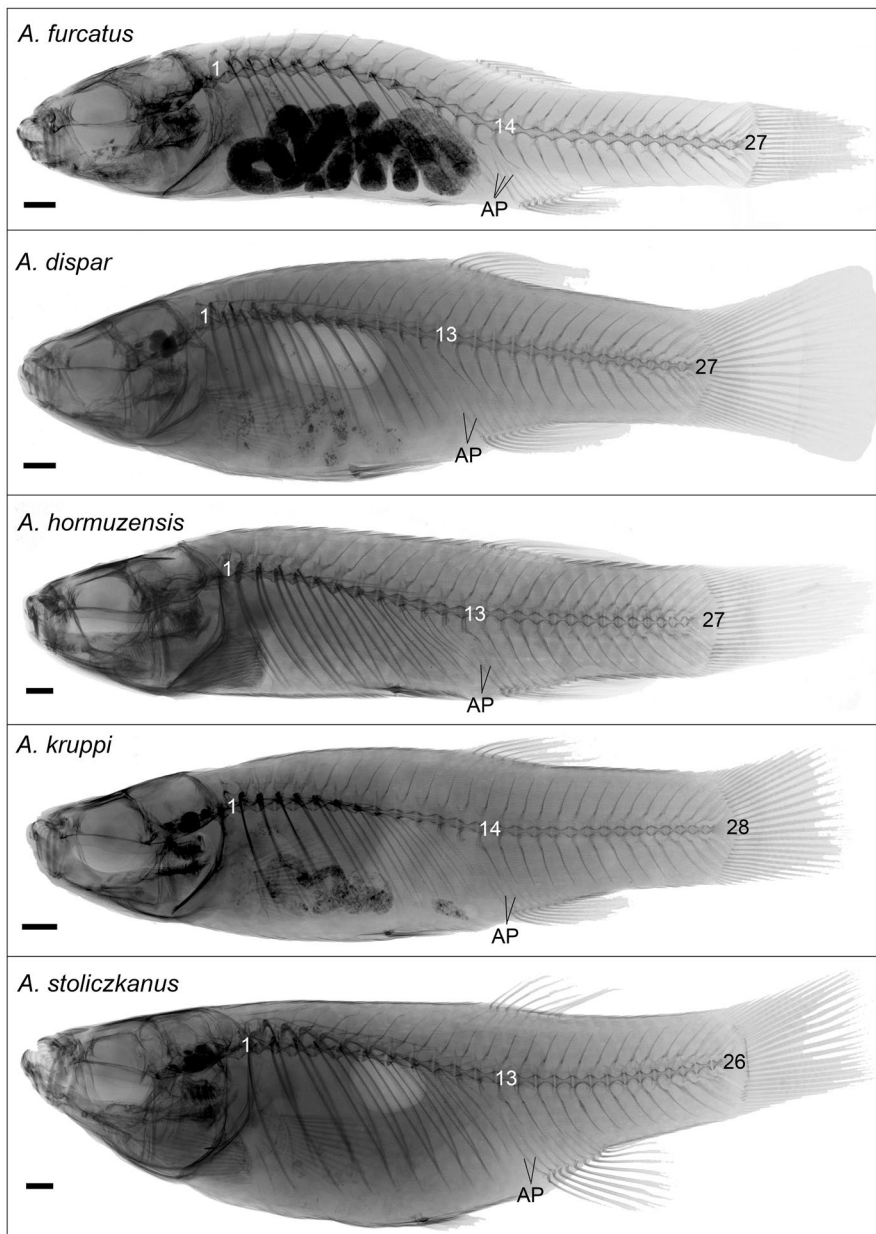
APPENDIX

FIGURE A1 X-ray images of *Aphaniops furcatus*, *A. dispar*, *A. hormuzensis*, *A. kruppi* and *A. stoliczkanus*. Numbers indicate the first abdominal vertebra, and the first and last caudal vertebra. AP depicts the anal fin pterygiophores anterior to the first haemal spine. Scale bars = 1 mm.